Synthesis and Characterization of Spiral Carbon Nanofibers Containing Pd Metal Cluster by Using $Pd_2(dba)_3$ as Catalyst

C.-J. Su [*], L.-S. Hsu [**], T.-W. Wu [**], C.-J. Liu [**], and S.-H. Lin [***]

[*] Department of Applied Chemistry, Chung Shan Medical University, Taichung, Taiwan, Republic of China, suru@csmu.edu.tw.
[**] Department of Physics and Graduate Institute of Opto-electronic Engineering, National Chang-Hua University of Education, Chang-Hua 50058, Taiwan, Republic of China, phhsu@cc.ncue.edu.tw.
[***] Institute of Atomic and Molecular Sciences, Academia Sinica, Taipei, Taiwan, Republic of China, hcshaw@po.iams.sinica.edu.tw.

ABSTRACT

The spiral carbon nanofibers consisting of Pd metal cluster were grown by the $Pd_2(dba)_3$-catalyzed decomposition of gaseous acetylene on molecular sieves (Linde 13X) support. The phase and composition of the sample was measured with x-ray diffraction (XRD). The microstructure and composition of the spiral carbon nanofibers were characterized by transmission electron microscope (TEM) and selective area diffraction (SAD). These Pd metal clusters show a small hysteresis from magnetization (M) vs. magnetic field (H) data and insulating behavior from electrical resistivity measurement. The thermopower (S) data shows metallic behavior from Pd cluster. This is the first report of incorporation of Pd nanoparticles inside carbon nanofibers.

Keywords: spiral carbon nanofibers, Pd metal cluster

1 INTRODUCTION

Recently, there has been extensive interest in the structure and morphology of carbon nanofibers prepared by the catalytic decomposition of gaseous hydrocarbon using various transition metals such as iron, cobalt, nickel, and some of their alloys [1-3]. These catalysts have been employed to engineer the conformation and crystalline perfection of carbon fibers and tubular structures of nano-sized dimensions [4]. These nanofibers were generally whisker-like tubular structures with diameters controlled by the size of the small metal particles. In addition to the straight tubes, several intricate shapes and structures including helices, cones, tori, and rings have been identified [5-7]. At higher structural level, strong inter-tube van der Waals (vdW) attraction can generate at least two kinds of self-assembled nanotubes: firstly, nanotubes can bunch together and leads to the rope formation [6]; secondly, upon the ultrasonic irradiation, the nanotubes may be self-folded into ring configurations [8] and stabilized by the vdW attraction. However, very few observations of the self-organization among helically coiled nanotubes have been reported. In this work, we report the preparation and characterization of the spiral carbon nanofibers consisting of Pd metal cluster.

2 EXPERIMENTS

The carbon nanofibers were synthesized using the Linde 13X (Strem) supported $Pd_2(dba)_3$ (Aldrich) catalyst, which was prepared by the impregnation method. The Linde 13 X molecule sieve has a pore size of 10Å. $Pd_2(dba)_3$ fine powder of 0.1g was dissolved in 10 ml distilled water and stirred for 10 min. at 70°C. One gram of microporous Linde 13X was then slowly added into the solution and stirred for 1 h. The mixture was ground to fine purple-gray powder (100 mesh) and drying in an oven at 120°C for 10 h. A ceramic boat containing 100 mg of catalyst was placed inside a quartz tube located in the central part of a tubular electric furnace. The catalyst was heated at a rate of 30°C min^{-1} from room temperature to 200°C in air and rinsed at 200°C for 3 h. The gas mixture (N_2=100 ml min^{-1}, C_2H_2=10 ml min^{-1}) was introduced for about 3 min before the sample was brought to the desired reaction temperature (700°C) at a rate of 30°C min^{-1}, and the reaction was allowed to proceed at 700°C for another 2 h. Afterward, the acetylene gas flow was stopped, and the reactor was cooled down to room temperature in flowing nitrogen (100 ml min^{-1}) for 16 h. The reaction product was collected as fine black powder from the ceramic boat. We should mention that the synthesis of spiral carbon nanofibers is very sensitive to the reaction temperature. Only within a narrow temperature range of 700°C have the spiral structures been observed by the current method of preparation. No spiral nanofiber was observed at 650°C; and at 750°C, very few spiral nanotubes were observed by TEM.

The structure and phase of the sample was examined by XRD using the Cu K_α radiation. The microstructure of the carbon nanofibers was studied with the aid of TEM (JOEL

JEM-2010, 200 kV, equipped with ISIS 300 Energy Dispersive X-ray analyzer) after sonicating the samples in ethanol for 1 h and dispersing a drop of solution over holey carbon grids. The as-prepared powders were cold-pressed and made into parallelepiped pellets without heat treatments. The M vs. H data were measured with a SQUID (superconducting quantum interference device) magnetometer. The electrical resistance measurements as a function of temperature were carried out using standard four-probe technique. Silver paste was applied to make the electrical contacts. A magnetic field of 5000 G was applied parallel to the current flow direction. The thermoelectric power is measured between 80 and 290 K. Thermopower data were only collected after the system reaches a steady state, which can be monitored from a user-written program. The temperature gradient across the sample was monitored using a Type E differential thermocouple.
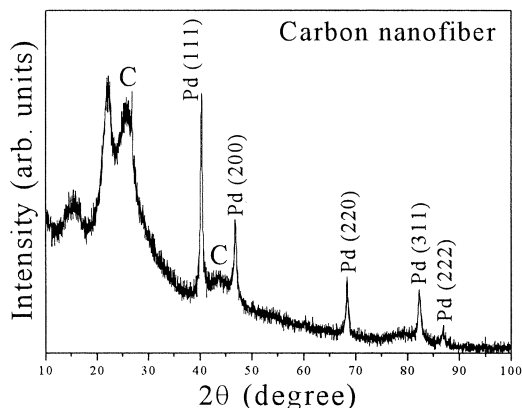
3 RESULTS AND DISCUSSION

Figure 1. X-ray diffraction data of carbon nanofibers containing Pd metal cluster.

The XRD pattern shown in Figure 1 shows the carbon broad structures at $2\theta=26$ and $44°$ and several low-indexed Pd peaks. These data confirm that the sample is carbon nanofibers consisting of Pd metal clusters. The broad C peaks show clearly the small particle size effect of the carbon nanofibers. The various Pd peaks assert that the Pd metal is in the form of metal clusters, not metal crystallites.

Besides the irregularly curved carbon nanotubes, the TEM image shown in Figure 2 clearly displays two types of spiral structure of the carbon nanofibers, which are distinguished according to their pitch (p) to diameter (2r) ratio, or equivalently, the pitch angle of the helix, $\varphi=\arctan(p/2\pi r)$ [9]. The p and 2r values of a typical type-I nanofiber in Figure 2 are found to be roughly 140 and 70 nm, respectively, which leads to $\varphi=32°$. A typical type-II nanofiber has p and 2r values of about 110 and 27 nm, respectively, which leads to a large pitch angle ($\varphi=52°$).
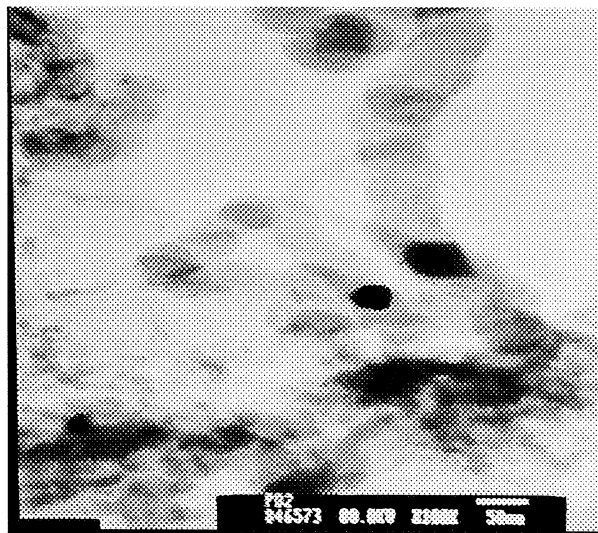

Figure 2. A TEM image showing three types of carbon nanofibers.

Most of the helices observed belong to type I nanofibers with low pitch angles. Since the low pitch-angle nanofibers appear to have larger vdW adhesive energy due to large contact area among different strands, it is proposed here that the vdW adhesive energy is the major factor for the stability of the spiral structure of the carbon nanofibers. More work is needed for a detailed understanding of the underlying physics. The slit width (13 nm) of the type-II carbon nanofiber has made it candidate material for hydrogen storage and high tensile strength composite. The SAD data show that the black spots inside the carbon nanofibers in Figure 2 are palladium metal (not PdO) clusters of diameters 40-60 nm. This observation strongly supports the successful incorporation of Pd metal clusters inside the carbon nanofibers in our syntheses processes.
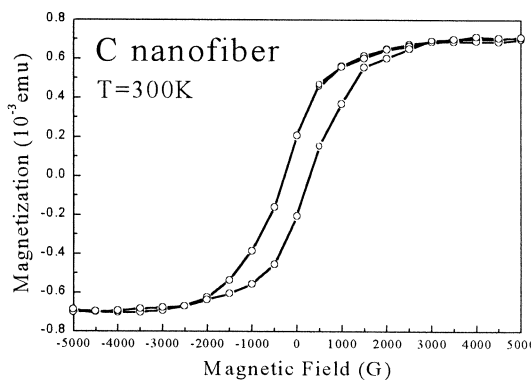

Figure 3. The magnetization vs. magnetic field curve of carbon nanofibers containing Pd metal cluster at temperature of 300K.

The M(H) curve at 300K for carbon nanofibers consisting of Pd metal cluster is shown in Figure 3. It is symmetric and the saturation magnetization is 7×10^{-4} emu. The coercive field and remanent magnetization is 300 G and 2×10^{-4} emu, respectively.
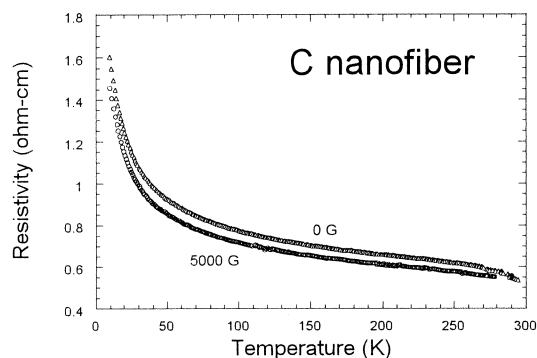

Figure 4. The electrical resistivity vs. temperature curve of carbon nanofibers containing Pd metal cluster in a magnetic field of 0 and 5000G.

As shown in Figure 4, the electrical resistivity of carbon nanofibers containing Pd metal cluster varies from 0.5 to 1.6 Ω cm for temperature between 10 and 300K. We note that the typical electrical resistivity value for the Pd metal at room temperature is 9.77 $\mu\Omega$ cm [10]. The insulating behavior from the electrical resistivity measurement indicates that the Pd metal cluster is enclosed inside the carbon nanofibers, which is also confirmed by TEM and SAD data. The nonmetallic temperature dependence of electrical resistivity could arise from the fact that there may be two types of nanofibers coexist, the conduction process of which could be described by a heterogeneous model. In a heterogeneous model, the total electrical resistivity ρ_T is given by [11]

$$\rho_T = \sum R_i \frac{A_i}{L_i}, \qquad (1)$$

where L_i is the fraction of sample length for the materials with electrical resistivity ρ_i, and A_i the corresponding fraction of sample cross-sectional area. The total electrical resistivity is then dominated by the more resistive inter-fibril contact barriers, which might account for the nonmetallic temperature-dependent behavior in our sample.

The material also shows a negative magnetoresistance (MR) effect upon applying a magnetic field of 5000 G. The MR ratio, defined as $[\rho(0G)-\rho(5000G)]/\rho(0G)$, is in the range of 5-10% and increases gradually with decreasing temperature. The maximum MR ratio is 10% at 10 K.

The S vs. T curve of carbon nanofibers containing Pd metal cluster is shown in Figure 5. The value of its thermopower is quite small and shows a remarkably linear
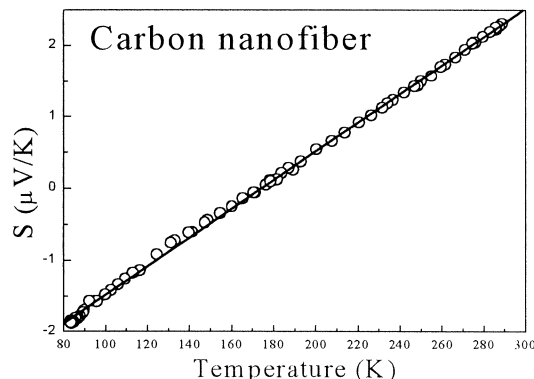

Figure 5. The thermoelectric power vs. temperature curve of carbon nanofibers containing Pd metal cluster.

behavior of temperature dependence. Note that the room-temperature thermopower on mats of single-wall carbon nanotubes are very large (in the range of 20-60 μV/K) and remains positive down to 4.2 K [12-14]. Above 174 K, the thermopower is positive and decreases with decreasing temperature. A sign crossover occurs below 174 K. This result suggests that there exists more than one type of carrier. There are at least two possibilities for the sign crossover: (1) The two types of carbon nanofibers consisting of Pd metal clusters have opposite sign of carriers; (2) The charge carriers of carbon nanofiber are holes (the same as the hole carriers in the mats of single-wall nanotubes), whereas the charge carriers of Pd metal clusters are electrons. The metallic diffusion thermopower of our material does not seem to reconcile with the nonmetallic behavior in the temperature dependence of its electrical resistivity. This may results from the fact that the inter-fibril contact barriers have little contribution to thermopower. According to Kohler's formula, the diffusion thermopower for a conductor made of i elements in series can be expressed as

$$S_D = \frac{\sum_i S_i W_i}{\sum_i W_i}, \qquad (2)$$

where S_i is the partial thermopower of the ith element, and W_i is the thermal resistivity. The inter-fibril contact barriers make our material showed nonmetallic behavior in the temperature dependence of the electrical resistivity, but the small weighting factor of thermal resistivity due to the inter-fibril contact barriers would not affect the metallic diffusion thermopower behavior.

The linear dependence of S with T shows the metallic behavior of the Pd cluster. For metallic conduction, S varies linearly with T [15], and the free-electron expression is [16]

$$S = (\frac{\pi^2 k_B^2 n(E_F)}{3Ne})T,$$ (3)

where N is the number of electrons per unit cell, e is the electron charge, k_B is Boltzmann's constant, and $n(E_F)$ is the density of states at the Fermi energy. The dashed line in Figure 5, which has a slope of 2×10^{-8} V/K^2, is the least-squares fit to the data points. Comparing with the equation (3) and using N=2, one determines that $n(E_F)$=1.64 electrons per eV per unit cell, which is comparable to the $n(E_F)$ value of Pd metal.

4 ACKNOWLEDGMENTS

REFERENCES

[1] M. S. Dresselhaus, G. Dresselhaus, and P. C. Eklund, "Science and Technology of Fullerenes and Carbon Nanotubes", Academic Press, San Diego, 1996.

[2] N. M. Rodriguez, J. Mater. Res. 8, 3233, 1993.

[3] M. Endo, K. Takeuchi, S. Igarashi, K. Kobori, M. Shiraishi, and H. W. Kroto, J. Phys. Chem. Solids 54, 1841, 1993.

[4] N. M. Rodriguez, A. Chambers, R. T. K. Baker, Langmuir 11, 3862, 1995.

[5] S. Amelinckx, X. B. Zhang, D. Bernaerts, X. F. Zhang, V. Ivanov, and J. B. Nagy, Science 265, 635, 1994.

[6] A. Thess, R. Lee, P. Nikolaev, H. Dai, P. Petit, J. Robert, C. Xu, Y. H. Lee, S. G. Kim, A. G. Rinzler, D. T. Colbert, G. E. Scuseria, D. Tomanek, J. E. Fischer, and R. E. Smalley, Science 273, 483, 1996.

[7] R. Gao, Z.-L. Wang, and S. Fan, J. Phys. Chem. 104, 1227, 2000.

[8] R. Martel, H. R. Shea, and P. Avouris, J. Phys. Chem. B 103, 7551, 1999.

[9] Z.-C. Ou-Yang, Z.-B. Su, and C.-L. Wang, Phys. Rev. Lett. 78, 4055, 1997.

[10] V. S. Egorov and I. N. Khlyustikov, "Handbook of Physical Quantities", edited by I. S. Grigoriev and E. Z. Meilikhov, p. 551, CRC Press, New York, 1997.

[11] A. B. Kaiser, G. U. Flanngan, D. M. Stewart, D. Beaglehole, Synthetic Metals 117, 67, 2001.

[12] M. Tian, F. Li, L. Chen, Z. Mao, Y. Zhang, Phys. Rev. B 58, 1166, 1998.

[13] L. G. Grogorian et. al., Phys. Rev. Let. 80, 5560, 1998.

[14] J. Hone et. al., Phys. Rev. Lett. 80, 1042, 1998.

[15] N. F. Mott and H. Jones, "The Theory of the Properties of Metals and Alloys", Chap. VII, Dover, New York, 1958.

[16] D. K. C. MacDonald, "Thermoelectricity: An Introduction to the Principles", pp. 25-26, John Wiley, New York, 1962.